agronomy

MDPI

Article

Particle Size Distribution and Depth to Bedrock of Chinese Cultivated Soils: Implications for Soil Classification and Management

Xiaoning Zhao [1,2,*], Wei He [1], Lihua Xue [2], Feng Chen [3,4], Pingping Jia [1], Yi Hu [1] and Kazem Zamanian [1,5,*]

1 School of Geographical Sciences, Nanjing University of Information Science and Technology, Nanjing 210044, China
2 Institute of Grain Crops, Xinjiang Academy of Agricultural Sciences, Urumqi 830091, China
3 Co-Innovation Center for the Sustainable Forestry in Southern China, Nanjing Forestry University, Nanjing 210037, China
4 Jiangsu Hydraulic Research Institute, Nanjing 210017, China
5 Institute of Soil Science, Leibniz University of Hannover, Herrenhäuser Straße 2, 30419 Hannover, Germany
* Correspondence: jasminezxnsx@msn.com (X.Z.); zamanians@yahoo.com (K.Z.)

Abstract: Although a number of studies have provided information on soil texture, soil classification, and depth to bedrock throughout China, few studies have combined this information, which is the basis for agricultural field management. A total of 81% of China's cultivated lands are distributed among the Middle–Lower Yangtze Plain (18.2%), arid and semiarid North China Plain (18.2%), Northeast Plain (17%), Huang-Huai-Hai Plain (16.1%), and Yunnan–Guizhou Plateau (11.6%). The Huang-Huai-Hai Plain has the highest density of agricultural land (58.5%) and the greatest depth to bedrock of cultivated land (243–402 m). The lowest cultivated depth to bedrock (4–84 m) is concentrated in the Sichuan Basin and its surrounding regions. The main cultivated soil types are Anthrosols, Fluvisols, Cambisols, Phaeozems, Luvisols, Kastanozems, Leptosols, and Acrisols, under the main topsoil texture classes of loam, clay loam, silty clay loam, silt loam, sandy loam, and clay. The Fluvisols had the largest depth to bedrock (156 m) on the Middle–Lower Yangtze Plain and Huang-Huai-Hai Plain, with the highest silt soil distributions but comparable lower sand contents. The Yunnan–Guizhou Plateau had the highest clay soil content. The cultivation under Kastanozems and Leptosols on the Qinghai–Tibet Plateau and in arid and semiarid North China and under Phaeozems on the Northeast Plain should be restricted and managed very cautiously facing erosion risk. The higher percentages of Anthrosols are on the Middle–Lower Yangtze Plain (37%), in Southern China (32%), and on the Yunnan–Guizhou Plateau (26%). The same cultivation aim (i.e., more crop 0production) has produced a similar range of properties over time among the soils developed on agricultural fields, which are classified as Anthrosols. However, various soil types can still be found in agroecosystems because of the variations in climate and topography. Our results highlight that the agriculture-based soil climate and topography shape the interaction of the soil development and not only the pedogenic history of the soil development under variations in the soil depth to bedrock but also the cultivation of distinct pedogenic features. This study provides cultivated soil information on the depth to bedrock, soil classification, and soil texture in China, as well as instructions for field strategies for sustainable agricultural development.

Keywords: agropedogenesis; land utility; soil taxonomy; environmental planning; global changes

check for updates

Citation: Zhao, X.; He, W.; Xue, L.; Chen, F.; Jia, P.; Hu, Y.; Zamanian, K. Particle Size Distribution and Depth to Bedrock of Chinese Cultivated Soils: Implications for Soil Classification and Management. *Agronomy* **2023**, *13*, 1248. https://doi.org/10.3390/agronomy13051248

Academic Editor: Jiafa Luo

Received: 29 March 2023
Revised: 24 April 2023
Accepted: 26 April 2023
Published: 27 April 2023

1. Introduction

The process of soil formation over time is controlled under natural conditions by organism activities, climate, parent materials, and topographic factors [1,2], and in agroecosystems particularly, by human interventions [3,4]. Agricultural soils exist objectively for use as the most basic means of agricultural production, for which the soil development direction is conscious, purposeful, and completely directional. This tends to weaken the structure and correlation of the spatial variation of the variables and the spatial heterogeneity of the soil properties, including the nutrient availability, which develops in a uniform direction [4].

Among the properties, the soil texture and rooting depth (i.e., depth to bedrock (or any hardpan)) are determinant in root proliferation and nutrient acquisition [5]. Soil texture is an important soil property that controls most of the physical, chemical, and biological processes in soils [6]. Soil texture often has high spatial heterogeneity along landscapes in both the lateral and vertical dimensions [7]. Currently, there is an increasing demand for detailed three-dimensional soil texture information [8] to deal with global and national issues, such as climate change, soil degradation, water resource shortages, environmental pollution, and agricultural and ecosystem sustainability [9–11]. The soil texture not only determines the quality of the soil tillage, but it also directly controls the soil structure, water permeability and retention, and drainage and ventilation rates, as well as the resistance against root penetration and the difficulty of tillage and land preparation [12,13]. Therefore, soil texture is important in soil fertility through the interactions of water, fertilizer, air, and heat [14,15].

Agricultural soils play an important role in the carbon cycle [16,17]. The soil quality and its health are related to the physical, chemical, and biological properties, which are not only naturally controlled by the local climatic and topographic conditions but are also decided by the land managers in agroecosystems [18]. In the current agricultural production regime, due to the excessive pursuit of crop yields by growers, chemical fertilizers, pesticides, and other amendments are excessively used [19,20], which may not only cause various environmental problems but also change the direction of the soil development towards anthropogenic soils [4]. Long-term fertilization may considerably change the soil's chemical [19], physical [21], and microbial properties [22]. For example, soil acidification is a common problem following long-term overfertilization and applications of fertilizer amounts that greatly exceed the demands of crops [19]. Accelerated soil acidification decreases the efficient use of land resources and thus crop production [20], as well as intensifying mineral weathering. The soil carbonate stocks, which buffer the soil pH over geological timescales, can be completely lost over just a few decades [23,24]. Therefore, understanding the formation and evolution of the spatial and temporal variation in soil properties is important not only for predicting the direction of soil development but also as a basis for the correct determination of the best field management in agricultural fields.

China has managed to feed 20% of the world's population with only 7% of the world's arable land [25]. Most studies usually use advanced machine learning methods, such as random forests and deep learning, and they focus on a combination of observed data and environment variables, such as temperature, precipitation, and topography, to obtain the spatial distribution of soil properties over various scales [26–28]. Although a number of studies have provided information on soil texture [29] and depth to bedrock [30] throughout China, few studies have combined this information with the soil types (i.e., soils with similar properties over defined depths). We explored the relationship between the soil types, soil texture, and soil depth to bedrock of cultivated land in the Chinese agricultural sector to assess how long-term agricultural practices control the soil development, and how the local climatic and topographic conditions may modify the rate of the soil development in agroecosystems. The objectives were to answer the following questions: (1) What is the particle size distribution and soil depth to bedrock of Chinese cultivated land? (2) How do the typical geographical characteristics and climate influence the rate of soil development on cultivated land?

2. Materials and Methods

2.1. Study Site

We selected the boundary data of nine agricultural zones provided by the Center for Resources and Environmental Science of the Chinese Academy of Sciences (https://www.

resdc.cn/Default.aspx) (accessed on 5 April 2022) (Figure 1a). The delineation of these agricultural zones group areas with similar agricultural inputs and intensities, important problems, and integrities of administrative units. The zones are as follows: the middle and lower reaches of the Yangtze River Plain (A); the Huang-Huai-Hai Plain (B); the Northeast Plain (C); the arid and semiarid North China Plain (D); the Loess Plateau (E); the Qinghai–Tibet Plateau (F); Southern China (G); the Yunnan–Guizhou Plateau (H); and Sichuan Basin and its surrounding areas (I) (Figure 1a).

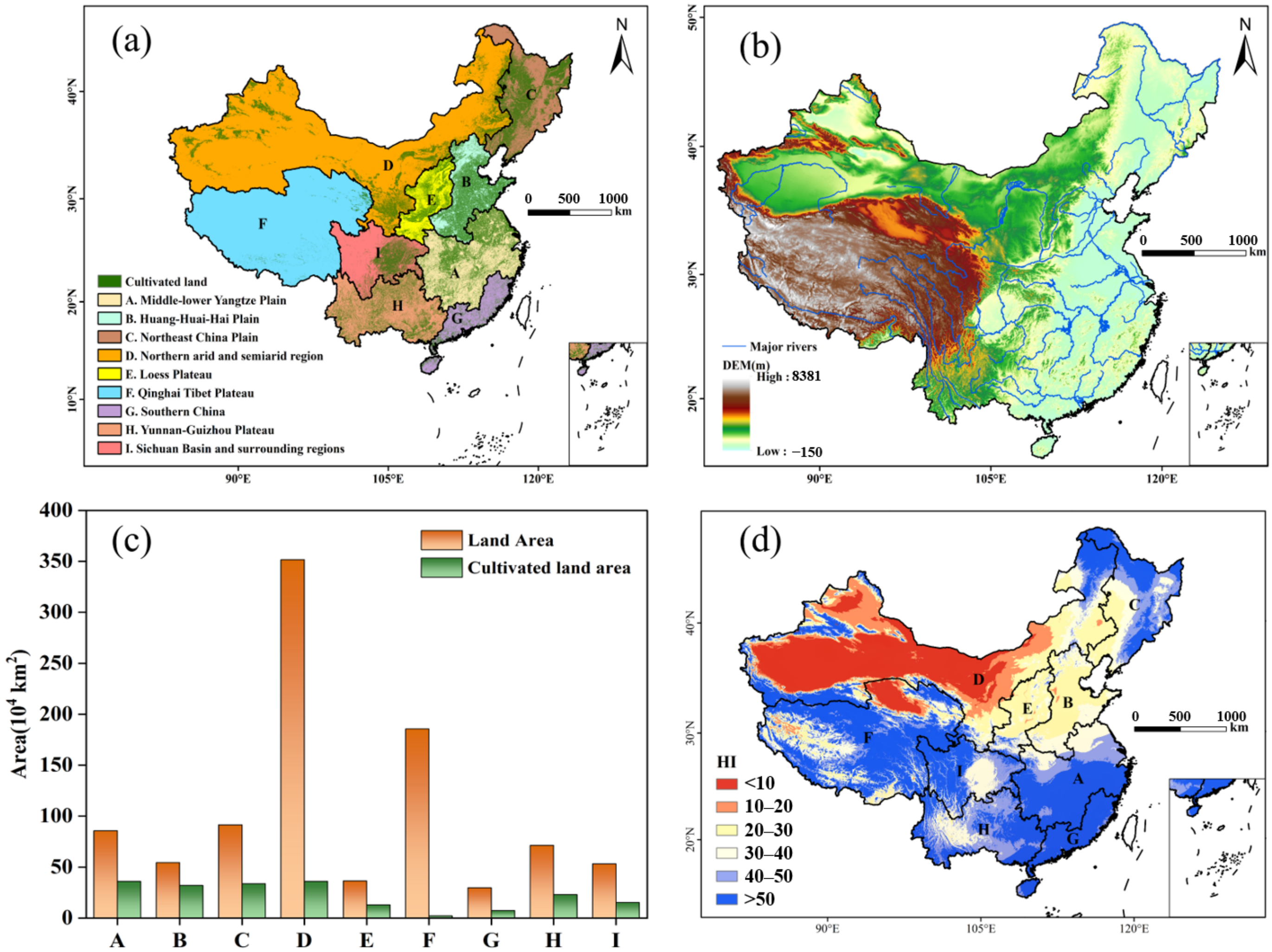

Figure 1. (**a**) Classification of cultivated lands depending on agricultural situation, characteristics, and development; (**b**) distribution of main water systems and digital elevation model (DEM); (**c**) total and cultivated land area ($\times 10^4$ km^2) of each cultivation zone in 2020; (**d**) distribution of humidity index (HI = MAP/(MAT + 10)) (MAP (mean annual precipitation) (mm) and MAT (mean annual temperature) (°C) from 1990 to 2015 in China). The weather data are from the Center for Resources and Environmental Sciences, the Chinese Academy of Sciences (https://www.resdc.cn/Default.aspx) (accessed on 5 April 2022). A: Middle–Lower Yangtze Plain; B: Huang-Huai-Hai Plain; C: Northeast China Plain; D: arid and semiarid North China Plain; E: Loess Plateau; F: Qinghai–Tibet Plateau; G: Southern China; H: Yunnan–Guizhou Plateau; I: Sichuan Basin and surrounding regions. The map is based on the standard map released by the Ministry of Natural Resources of the People's Republic of China (No. GS (2019) 1822).

2.2. Data

The remote sensing monitoring data of cultivated land with a 30 m spatial resolution for 2020 were provided by the Chinese Department of Natural Resources (http://www.

globallandcover.com) (accessed on 8 May 2022) and were resampled to 1 km in this study. The soil type data are from the National Tibetan Plateau Data Center based on the Harmonized World Soil Database (http://data.tpdc.ac.cn/zh-hans/) (accessed on 15 May 2022). HSWD V1.2 provided a raster map with a spatial resolution of 1 km, and the soil type was determined according to FAO-90. Soil depth-to-bedrock data were collected from Yan, 2020 [30]. The dataset was based on about 6382 drilling record observations, using random forests and the gradient propulsion tree algorithm space prediction model with a spatial resolution of 1 km. The soil texture data were collected from the basic attribute dataset of China's high-resolution National Soil Information Network provided by the National Earth System Science Data Center (http://www.geodata.cn) (accessed on 20 February 2022), with a spatial resolution of 1 km. The considered soil properties were the bulk density (g/cm^3) and the sand, silt, and clay contents (g/kg) in the topsoil (0–30 cm).

2.3. Data Analysis

According to the depth to bedrock and cultivated area of each soil type (FAO-90) in the agricultural zones, the weighted average depth to bedrock of cultivated soils was calculated by Equation (1):

$$d = \frac{d_1 f_1 + d_2 f_2 + \ldots + d_{1n} f_n}{n} \quad (1)$$

where d is the weighted average depth to bedrock of cultivated soils; d_1, d_2 ... d_n are the average depths to bedrock of any of the cultivated soil types in the agricultural zones; f_1, f_2 ... f_n are the weights for each of the cultivated soil types; and n is the number of soil types.

The dataset of China's high-resolution National Soil Information Network provided soil particle size distribution data at topsoil depths of 0–5, 5–15, and 15–30 cm. The percentages of sand, silt, and clay were calculated by the weights of the sand, silt, and clay divided by the weight of the sand, silt, and clay of the topsoil (0–30 cm).

3. Results

3.1. Distribution of Cultivated Land in Agricultural Zones

A total of 81% of China's cultivated land in 2020 was distributed among five agricultural zones as follows: the Middle–Lower Yangtze Plain (18.2%) (A) = arid and semiarid region North China Plain (18.2%) (D) > Northeast Plain (17%) (C) > Huang-Huai-Hai Plain (16.1%) (B) > Yunnan–Guizhou Plateau (11.6%) (H) (Figure 1a, d). The rest of the cultivated land (18.9%) was distributed among the Sichuan Basin and its surrounding regions (7.7%) (I), the Loess Plateau (6.5%) (E), Southern China (3.7%) (G), and the Qinghai–Tibet Plateau (1%) (F) (Figure 1a, d). The Huang-Huai-Hai Plain (B) had the highest density of agricultural land (58.5%) (Figure 1c), while the lowest density was on the Qinghai–Tibet Plateau (F) (1%). The density of agricultural land was 10.2% on the arid and semiarid North China Plain (D) (Figure 1c).

3.2. Depth Distribution of Cultivated Soils in Relation to Soil Types

The largest depth to bedrock of cultivated land was on the Huang-Huai-Hai Plain (B) (20–192 m) (i.e., the river estuary to the Bohai Sea), followed by the Middle–Lower Yangtze Plain (A) (0–149 m) near the coastal plain in A and the Huai He River Basin in B (Figure 2). Depths to bedrock of cultivated land of 20–95 m were found in the main river bends in A, B, C, D, and E. The rest of the zones, Southern China (G), the Yunnan–Guizhou Plateau (H), and the Qinghai–Tibet Plateau (F), had lower depths to bedrock of 6–87 m. The lowest depths to bedrock (8–23 m) were concentrated in the Sichuan Basin and its surrounding regions (I) (Figure 2).

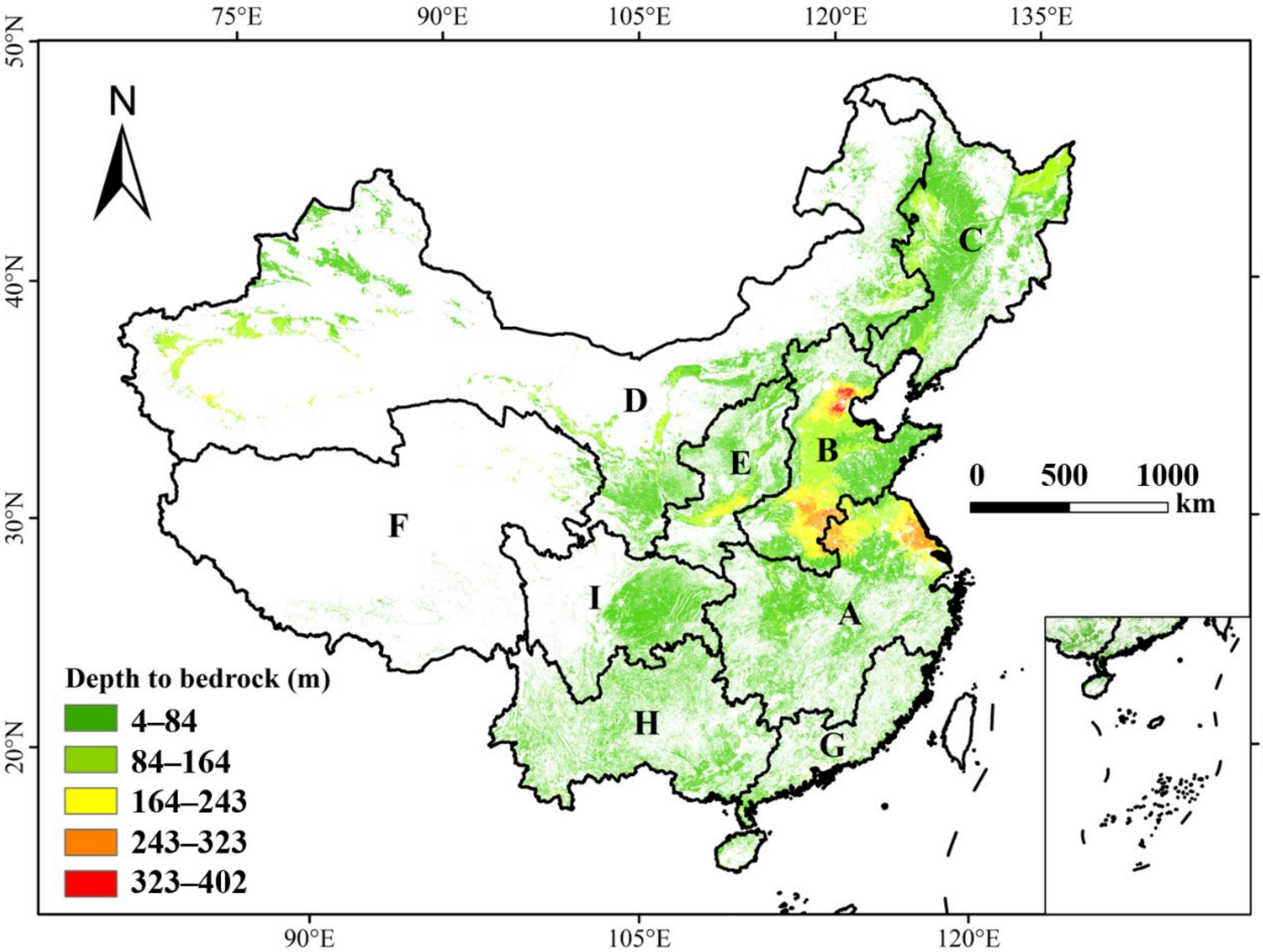

Figure 2. Depths to bedrock (m) of cultivated soils in nine agricultural zones of China. The data were sourced from Yan (2020) and modified. White color means no cultivated land or available data. The map is based on the standard map released by the Ministry of Natural Resources of the People's Republic of China (No. GS (2019) 1822).

The weighted averages of the depths to bedrock could be grouped as follows: Group 1 including soils in A and B with 70–110 m > Group 2 including soils in C, D, E, and F with 40–60 m > Group 3 including soils in G, H, and I with 15–35 m (Figure 3, right). The Fluvisols in A and B showed the largest depth to bedrock at 156 m, while the Cambisols in I had the shallowest depth to bedrock at 15 m. Fluvisols generally had the greatest soil depths to bedrock in cultivation zones A and B (156 m) and D (72 m), while Luvisols (27 m in C; 16 m in H) and Acrisols (22 m in G and H) were among the soils with the shallowest. Cambisols had the largest range of soil depth to bedrock: from 15 to 62 m (62 m in B; 41 m in D; 48 m in E; 22 m in H; 15 m in I). Anthrosols were in all zones except for B and C, with higher percentages of total cultivated area in A (37%), G (32%), and I (26%). Anthrosols were generally between 19 and 81 m deep (19 m in I; 38 m in G; 59 m in A; 81 m in D), except in zone E, where their depth was about 120 m. The soil depths to bedrock of Kastanozems (33 m in D; 49 m in F), Phaeozems (45 m in C), and Leptosols (39 m in F) were from 33 to 49 m.

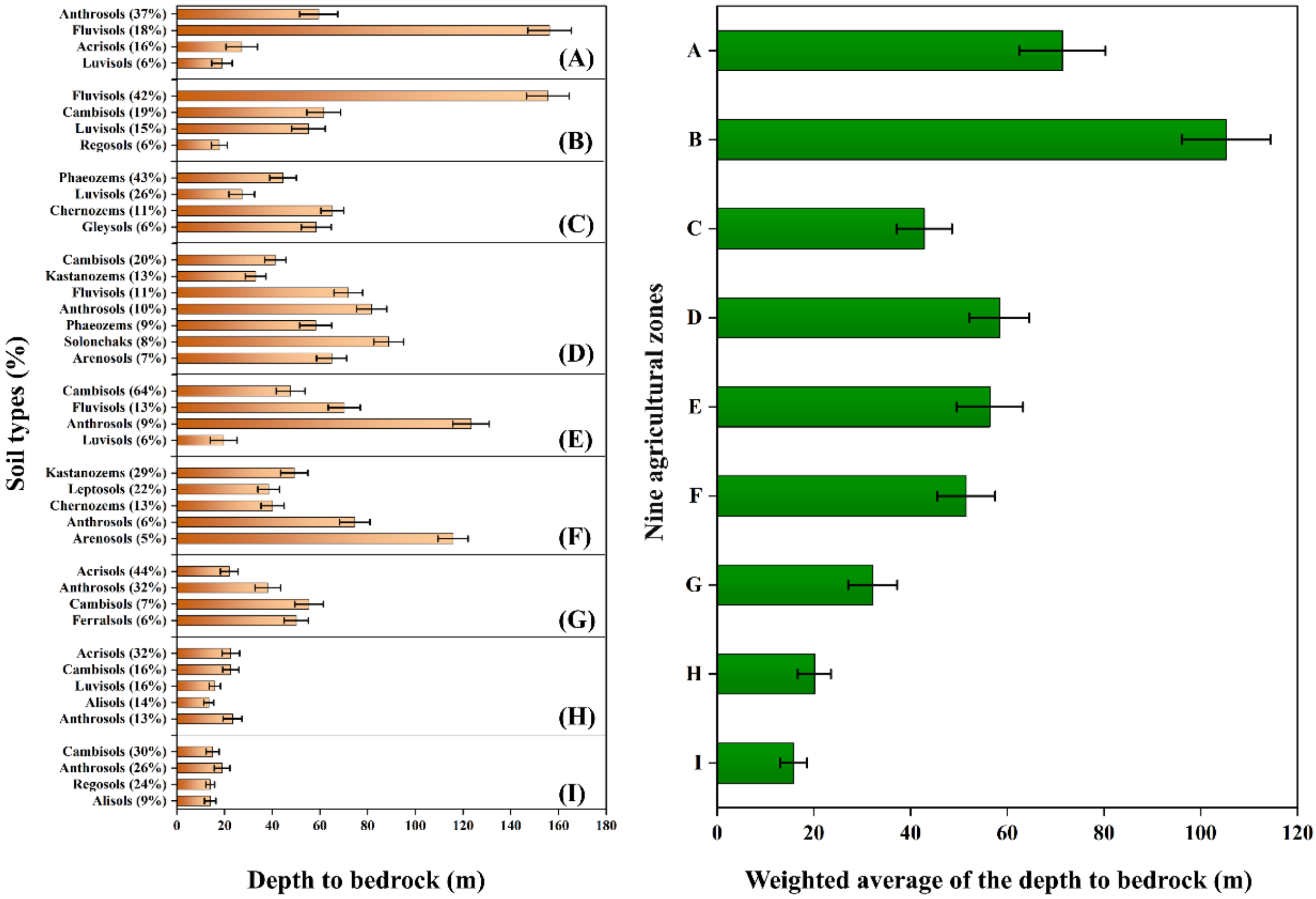

Figure 3. Depths to bedrock (m) of main cultivated soil types according to the percentage of land area (in brackets on *X* axis) in each agricultural zone (left), and weighted averages of the depths to bedrock of main cultivated land soil types in agricultural zones (right). (**A**): Middle–Lower Yangtze Plain; (**B**): Huang–Huai–Hai Plain; (**C**): Northeast China Plain; (**D**): arid and semiarid North China Plain; (**E**): Loess Plateau; (**F**): Qinghai–Tibet Plateau; (**G**): Southern China; (**H**): Yunnan–Guizhou Plateau; (**I**): Sichuan Basin and surrounding regions. The depth–to–bedrock data were sourced from Yan (2020) and modified.

3.3. Particle Size Distribution of Cultivated Soils in Agricultural Zones

The 20–40% sand content had the highest proportion (57%) in the cultivated soils (Figure 4a). Sandy cultivated soil was found in A, C, D, G, and I, where alluvial plains, basins, and islands are located (Figure 4d). The Sichuan Basin in zone I, alluvial plain of the Songnen Plain in C and D, the Liaohe Plain in D, the Tarim River Basin in D, Hainan Island in G, and the Pearl River Basin in G had the highest sand contents. The 20–30% clay content had the highest proportion (43%) (Figure 4b). The highest clay content (40–56%) was in H. The clay soil in the cultivated land was mainly concentrated in A and H, where the Huaihe River Basin and Yunnan–Guizhou Plateau are located (Figure 4d). The 40–60% silt content had the highest proportion (60%). The highest silt contents (80–90%) and silty cultivated soils were in A, B, C, D, and E, including the coastal plains in A, the Hai He River Basin in B, the Junggar Basin in D, the Wei He River Basin in D and E, and the Songhua and Liaohe river basins in C (Figure 4c,d).

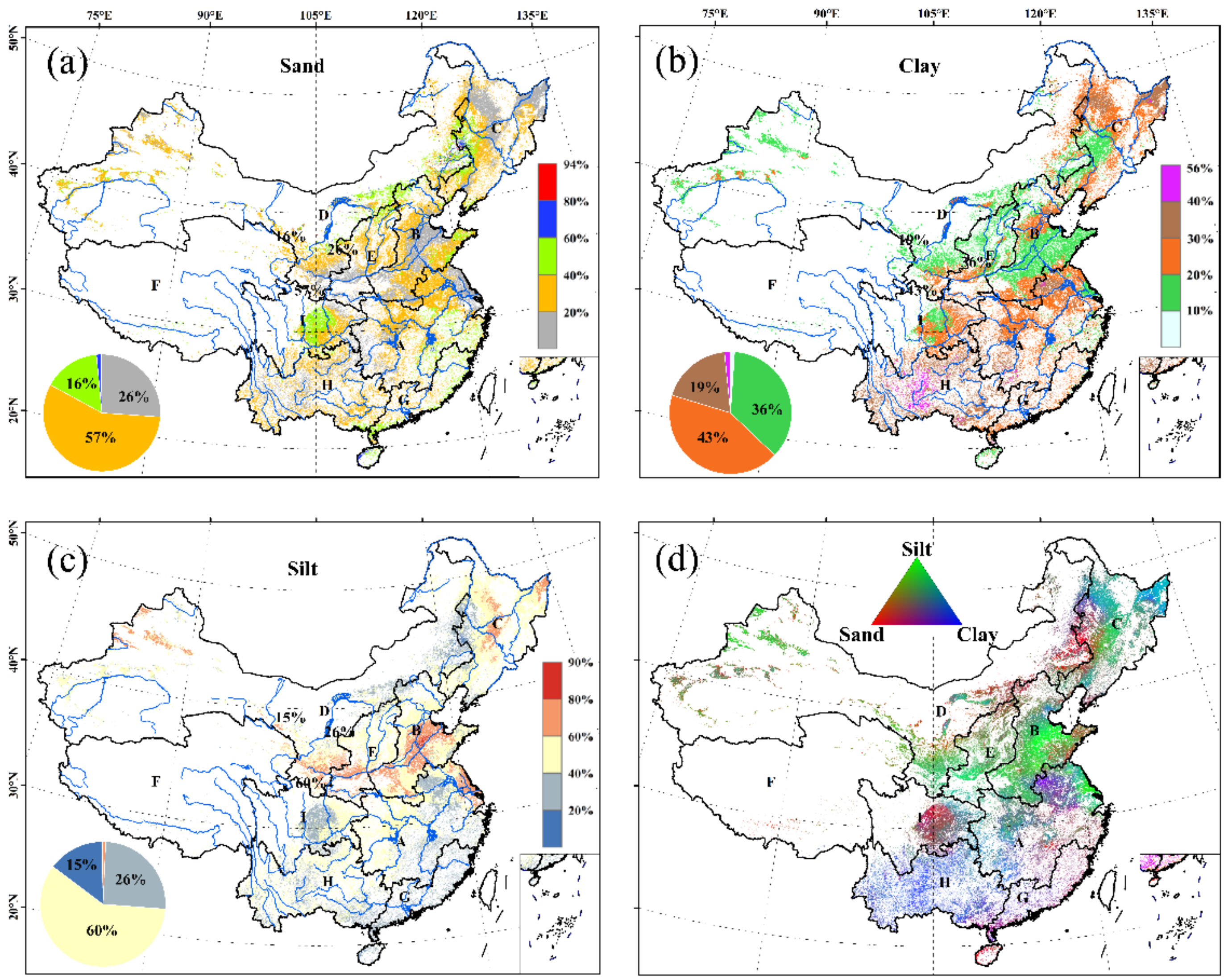

Figure 4. Distribution of (**a**) sand, (**b**) clay, and (**c**) silt, and (**d**) textural class of topsoil (0–30 cm) in cultivated areas of 9 agricultural zones in China. Color intensities in (**d**) indicate various soil textures. The pie chart on the left side of each figure indicates the areas of corresponding classes of (**a**) sand, (**b**) clay, and (**c**) silt. The data were sourced from Liu (2021) and modified. White color means no cultivated land or available data. The map is based on the standard map released by the Ministry of Natural Resources of the People's Republic of China (No. GS (2019) 1822).

The main cultivated soil types are Anthrosols, Fluvisols, Cambisols, Phaeozems, Luvisols, Kastanozems, Leptosols, and Acrisols, with the main topsoil textures of loam, clay loam, silty clay loam, silt loam, sandy loam, and clay (Figure 5). The Fluvisols are mainly silt loam in B (84%) and A and D (44–47%), clay loam in A (33%), and loam in D (45%). The Luvisols are loam (38%) and silt loam (38%) in C. The Kastanozems are mainly loam (68%) and sandy loam (15%) in D but silt loam (94%) in F. The Leptosols are mainly loam (44%), sandy loam (28%), and silt loam (28%) in F. The Phaeozems are mainly silt loam (36%), silty clay loam (36%), and loam (19%) in C. The Acrisols are clay loam in G (52%) and H (75%) and loam in G (36%). The Cambisols are mainly silt loam in B, D, I, and E (60–73%); loam in B, D, and E (19–32%); clay loam in H and I (22–45%); and clay and silty clay loam (23%) in H. The Anthrosols have a wide particle size distribution, with 75% loam and 10% sandy loam in I, 69% silt loam and 24% loam in D, and 52% clay loam and 35.6% loam in G (Figure 5).

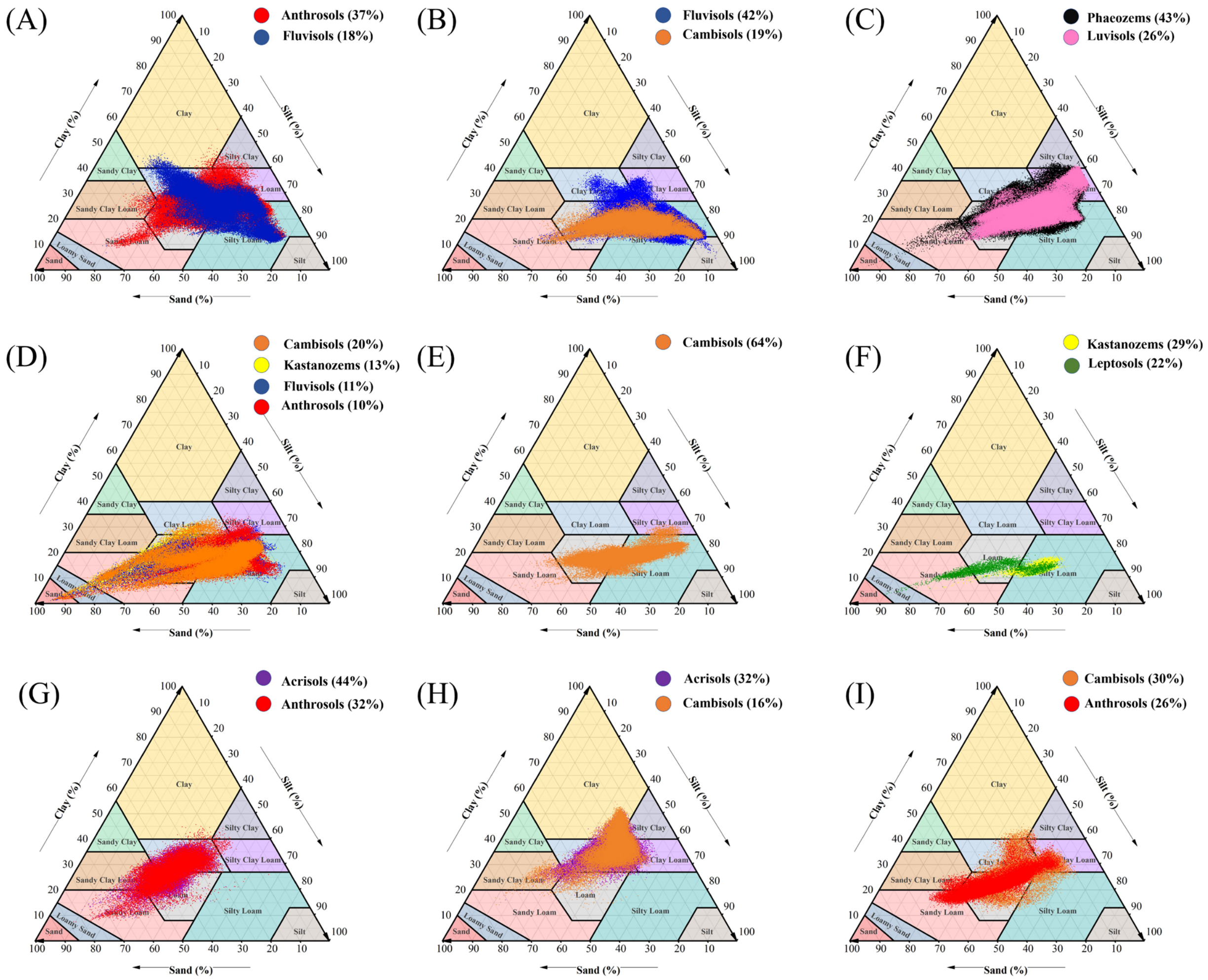

Figure 5. Ternary diagram of cultivated soil textures of main soil types (>50%) in different agricultural zones. (**A**) Middle–Lower Yangtze Plain; (**B**) Huang-Huai-Hai Plain; (**C**) Northeast China Plain; (**D**) arid and semiarid North China Plain; (**E**) Loess Plateau; (**F**) Qinghai–Tibet Plateau; (**G**) Southern China; (**H**) Yunnan–Guizhou Plateau; (**I**) Sichuan Basin and surrounding regions.

4. Discussion

4.1. Factor Effects on Cultivated Soil Development

Combining the texture data with the soil type data, the soil texture is strongly controlled by topographic and climatic factors. In the extreme weathered soils of the humid climate in H and G, there were Acrisols with the highest clay content (30%) but shallowest depth to bedrock (Figures 4 and 5). The Acrisols in H and G had similar soil depths to bedrock but with less clay content in G than H, which had the highest clay content (40–56%) (Figure 4). The soil of G has less clay content because of the topography of the Yunnan–Guizhou Plateau in H and Pearl River Basin in G, where the river basin has more sand (Figure 4). Taking the agricultural areas G, H, and I as an example, the climate in these areas is humid, with high temperatures and strong mineral weathering potential. From the perspective of various types of stickiness and their occurrence conditions, the humidity in this area is relatively high, and secondary stickiness is generally not possible, while residual stickiness may be the main reason for the heavy soil texture in this area. The residual argillification is closely related to the desilication and iron-rich aluminization in this region, which lead to the decomposition of primary soil minerals through desalination and desilication, initially forming 2:1-type clay minerals but further transforming into 1:1-type clay minerals and iron aluminum oxides. Soil cementation (the soil becomes sticky) gradually increases with desilication and iron-rich aluminization [31]. On the alluvial plains in A and

B, the greatest depths in the Fluvisols are because of the fluvial material accumulation of the two main Chinese rivers, the Yellow River and Yangtze River. The higher clay content in the Fluvisols of A than B is due to the topography of the Huang-Huai-Hai Plain in A and the Huan He River Basin in B, although under a similar climate. The climate and topography induced the Kastanozems, which are mainly loam and sandy loam in the northern arid and semiarid area but silt loam in Tibet.

The same cultivation aim (i.e., more crop production) has produced a similar range of properties over time among the soils developed on agricultural fields, which are classified as Anthrosols. However, variations in the climate, topography, and parent material may lessen or intensify the rate of change in the properties of the agricultural soils. Therefore, after centuries of cultivation, various soil types can still be found in agroecosystems. On the Northeast China Plain (C), the cultivation was conducted on the humus-rich Phaeozems and Luvisols following land use change from forests or grasslands over the past 30 years. Similarly, on the Huang-Huai-Hai Plain (B), about 76% of the soils are Fluvisols, Cambisols, and Luvisols because the fluvial humus reaches these soils. Deeper depths to the bedrock of the Kastanozems were found on the Tibet Plateau compared with the northern arid and semiarid regions, and the relatively lower SOM content in the topsoil and harsh climatic conditions have limited the suitability of these soils for agricultural purposes [32]. Furthermore, soil erosion is a considerable threat that causes the loss of topsoil following land use change [33]. Fluvisols were the dominant soil types in B, A, and D, where fluvial materials produce the deepest soils near rivers or lakes and in deltaic areas. Acrisols are the main dominant soil types in G and H, where acidity and the leaching of base cations are the main problems for cultivation.

4.2. Soil Classification Development for Cultivated Land Use

Variations in the climate, topography, and parent material, as well as the initial state of the soil development before cropping and the cultivation duration, may lessen or intensify the rate of change in the properties of agricultural soils [34]. Therefore, after decades to centuries of cultivation, the diagnostic horizons of Anthrosols, such as the irragric or hortic horizons, are absent, and various other soil types can be found in Chinese agroecosystems. For example, in the tropical and subtropical areas of the Yunnan–Guizhou Plateau (G) and Pearl River Basin (H), erosion has brought the subsoil clayey horizons to the surface, and the extreme leaching condition accompanying the presence of short-range-order clay minerals has prevented the accumulation of base cations in the soils, despite long-term fertilization and liming [35–37]. Therefore, the base saturation is still below 50% in these soils. In contrast, on the Huang-Huai-Hai Plain (B), river flooding is an active process [38], and about 76% of the soils are affected by the fluvial silt and humus sediments (Figure 5). Therefore, the prerequisite of the irragric horizon (i.e., less than 20% difference among soil particles) is violated, as the topsoil may even have up to 90% silt (Figure 5) (IUSS). A similar condition is also observable along the coasts and river basins in the other cultivated areas, such as the coastal plains in A [39] and the Liao River Basin in C. On the Northeast China Plain (C), the cultivation duration occasionally seems to be the main reason for the classification of soils in groups other than Anthrosols. In such areas, cultivation has begun over the past 30 years on the humus-rich Phaeozems and Luvisols following the clear-cutting of forests and grasslands [40]. Therefore, the relatively high soil fertility has negated fertilization, which may continue in the following decades. In short, despite considerable human interventions in agricultural fields, other soil-forming factors, such as topography, may still prevent the classification of such soils as Anthrosols [41]. We suggest that all the agricultural soils should be considered Anthrosols, regardless of the formation of specific diagnostic horizons, such as the irragric. This is because of the various consequences that agroecosystems have, such as for biodiversity [42], the loss of base cations [43], and environmental pollution [44]. Furthermore, the FAO-90 system is used in many countries as a basis for managing decisions [45,46], even though it is solely provided as a bridge among national classification systems [34]. In this regard, the addition of information on texture and depth to bedrock may provide further soil exploitation possibilities regarding, for example, rooting space and the utility of nutrients at deeper depths [47] and C sequestration below ground, as well as the opportunity to manage the leached nutrients and pollutants before they reach groundwater.

Due to long-term cultivation, various soil types other than Anthrosols can be found in agroecosystems. We combined the soil particle size distribution, depth to bedrock, and soil taxonomic classes of cultivated soils throughout China to assess how variations in climate and topography may prevent or lessen the development of agricultural soils toward Anthrosols. Texture was chosen because of the general belief in its dependency on the parent material and the determinant role of particle size distribution for the other properties. The depth to bedrock also has various environmental functions, such as space for carbon sequestration, especially when the groundwater is relatively deep. Our results show that not only erosion but also sedimentation are important factors that prevent the formation of the irragric or other diagnostic horizons of Anthrosols. In addition, topography and climate seem to be more effective on the soil particle size distribution than the parent material, negating the necessary condition of the <20% difference among the particle size classes of Anthrosols.

5. Conclusions

To explain the situation of the particle size distribution and soil depth to bedrock of Chinese cultivated land under different soil types and reveal the soil development of the cultivated land, we combined information on the soil texture, soil classification, and depth to bedrock throughout China using the remote sensing monitoring data of cultivated land from China's newly released high-resolution National Soil Information Grid dataset, soil data from the Harmonized World Soil Database, and soil depth-to-bedrock data. Our results showed that the Middle–Lower Yangtze Plain (A), arid and semiarid North China Plain (D), Northeast Plain (C), and Huang-Huai-Hai Plain (B) had higher cultivated land (>16%) compared with the other areas. B had the highest density of agricultural land (58.5%) and the greatest depth to bedrock of cultivated land (243–402 m), while the lowest density was on the Qinghai–Tibet Plateau (F) (1%), and the lowest cultivated depth-to-bedrock (4–84 m) zones were concentrated in the Sichuan Basin and its surrounding regions (I). The main cultivated soil types were Anthrosols, Fluvisols, Cambisols, Phaeozems, Luvisols, Kastanozems, Leptosols, and Acrisols. The Fluvisols in A and B showed the greatest depth to bedrock at 156 m, while the Cambisols in I had the shallowest depth to bedrock at 15 m. There was the highest silt soil distribution but comparable lower sand contents in A and B, and the highest clay soil content was on the Yunnan–Guizhou Plateau (H). The cultivation under Kastanozems and Leptosols in F and D and under Phaeozems in C should be restricted and managed very cautiously facing erosion risk. After long-term cultivation, the Anthrosols developed fast and had higher occupations in A (37%), D (10%), E (9%), F (6%), G (13%), and I (26%). Anthrosols have a wide particle size distribution with loam in I (75%) and A, D, and G (24–34%); clay loam in A and G (32–49%); loam in G (30%); silt clay loam (13%) in A; sandy loam in I (10%); and silt loam in D (69%). The agriculture-based soil climate and topography have shaped not only the pedogenic history of the soil development under variations in the soil depth to bedrock but also cultivated distinct pedogenic features. Our results provide cultivated soil information on the depth to bedrock, soil classification, soil texture, and sustainable agricultural development in China, and they highlight that the agriculture-based soil climate and topography shape the interaction of the soil development.

Author Contributions: X.Z.; funding acquisition, acquisition of data, analysis and interpretation of data, writing—original draft, visualization. W.H.; acquisition of data, writing—review and editing. L.X.; acquisition of data, formal analysis, validation. F.C.; writing—review and editing, formal analysis. P.J.; writing—review and editing. Y.H.; review and editing. K.Z.; funding acquisition, writing—review and editing. All authors have read and agreed to the published version of the manuscript.

Funding: This research was funded by the Jiangsu Specially Appointed Professor Project (grant number R2020T29); the National Natural Science Foundation of China (grant numbers 41877109, 32060433, 42050410320); and research Funds of Jiangsu Hydraulic Research Institute (grant number 2022Z019).

Conflicts of Interest: The authors declare no conflict of interest.

References

1. Jenny, H. *Factors of Soil Formation: A System of Quantitative Pedology*; McGraw-Hill Book Company Inc.: New York, NY, USA, 1941.
2. Roy, W.S. Factors of soil formation. A system of quantitative pedology. *Geoderma* **1994**, *68*, 334–335.
3. Dror, I.; Yaron, B.; Berkowitz, B. The Human Impact on All Soil-Forming Factors during the Anthropocene. *ACS Environ. Au* **2021**, *2*, 11–19. [CrossRef] [PubMed]
4. Kuzyakov, Y.; Zamanian, K. Reviews and syntheses: Agropedogenesis—Humankind as the sixth soil-forming factor and attractors of agricultural soil degradation. *Biogeosciences* **2019**, *16*, 4783–4803. [CrossRef]
5. Pérez, F.L. Biogeomorphic influence of soil depth to bedrock, volcanic ash soils, and surface tephra on silversword distribution, Haleakalā Crater (Maui, Hawai'i). *Geomorphology* **2015**, *243*, 75–86. [CrossRef]
6. Bresler, E.; Dagan, G.; Wagenet, R.J.; Laufer, A. Statistical Analysis of Salinity and Texture Effects on Spatial Variability of Soil Hydraulic Conductivity. *Soil Sci. Soc. Am. J.* **1984**, *48*, 16–25. [CrossRef]
7. Seaton, F.M.; George, P.B.; Lebron, I.; Jones, D.L.; Creer, S.; Robinson, D.A. Soil textural heterogeneity impacts bacterial but not fungal diversity. *Soil Biol. Biochem.* **2020**, *144*, 107766. [CrossRef]
8. Liu, F.; Zhang, G.-L.; Song, X.; Li, D.; Zhao, Y.; Yang, J.; Wu, H.; Yang, F. High-resolution and three-dimensional mapping of soil texture of China. *Geoderma* **2020**, *361*, 114061. [CrossRef]
9. Montanarella, L.; Vargas, R. Global governance of soil resources as a necessary condition for sustainable development. *Curr. Opin. Environ. Sustain.* **2012**, *4*, 559–564. [CrossRef]
10. Padarian, J.; Minasny, B.; McBratney, A.B. Chile and the Chilean soil grid: A contribution to GlobalSoilMap. *Geoderma Reg.* **2017**, *9*, 17–28. [CrossRef]
11. Rossel, R.A.V.; Chen, C.; Grundy, M.; Searle, R.; Clifford, D.; Campbell, P.H. The Australian three-dimensional soil grid: Australia's contribution to the GlobalSoilMap project. *Soil Res.* **2015**, *53*, 845–864. [CrossRef]
12. Radziuk, H.; Świtoniak, M. The effect of erosional transformation of soil cover on the stability of soil aggregates within Young Hummocky Moraine Landscapes in Northern Poland. *Agronomy* **2022**, *12*, 2595. [CrossRef]
13. Le Bissonnais, Y. Aggregate stability and assessment of soil crustability and erodibility: I. Theory and methodology. *Eur. J. Soil Sci.* **1996**, *47*, 425–437. [CrossRef]
14. Martín, M.Á.; Reyes, M.; Taguas, F.J. Estimating soil bulk density with information metrics of soil texture. *Geoderma* **2017**, *287*, 66–70. [CrossRef]
15. Ruggeri, R.; Tolomio, M.; Muganu, M.; Loreti, P.; Virga, G.; Iacuzzi, N.; Rossini, F. Establishment of a commercial organic hopyard in a Mediterranean environment: Production attributes and their relationship with soil texture. *Sci. Hortic.* **2023**, *310*, 111720. [CrossRef]
16. Li, X.; Feng, Y.J. *Carbon Sequestration Potentials in Agricultural Soils*; Alberta Research Council Inc.: Edmonton, AB, Canada, 2002.
17. Sun, W.; Huang, Y.; Zhang, W.; Yu, Y. Carbon sequestration and its potential in agricultural soils of China. *Glob. Biogeochem. Cycles* **2010**, *24*, 1–12. [CrossRef]
18. Doran, J.W. Soil health and global sustainability: Translating science into practice. *Agric. Ecosyst. Environ.* **2002**, *88*, 119–127. [CrossRef]
19. Jia, S.; Yuan, D.; Li, W.; He, W.; Raza, S.; Kuzyakov, Y.; Zamanian, K.; Zhao, X. Soil Chemical Properties Depending on Fertilization and Management in China: A Meta-Analysis. *Agronomy* **2022**, *12*, 2501. [CrossRef]
20. Yang, Z.; Hu, Y.; Zhang, S.; Raza, S.; Wei, X.; Zhao, X. The Thresholds and Management of Irrigation and Fertilization Earning Yields and Water Use Efficiency in Maize, Wheat, and Rice in China: A Meta-Analysis (1990–2020). *Agronomy* **2022**, *12*, 709. [CrossRef]
21. Pernes-Debuyser, A.; Tessier, D. Soil physical properties affected by long-term fertilization. *Eur. J. Soil Sci.* **2004**, *55*, 505–512. [CrossRef]
22. Morugán-Coronado, A.; Pérez-Rodríguez, P.; Insolia, E.; Soto-Gómez, D.; Fernández-Calviño, D.; Zornoza, R. The impact of crop diversification, tillage and fertilization type on soil total microbial, fungal and bacterial abundance: A worldwide meta-analysis of agricultural sites. *Agric. Ecosyst. Environ.* **2022**, *329*, 107867. [CrossRef]
23. Zhao, Y.; Wang, M.; Hu, S.; Zhang, X.; Ouyang, Z.; Zhang, G.; Huang, B.; Zhao, S.; Wu, J.; Xie, D.; et al. Economics- and policy-driven organic carbon input enhancement dominates soil organic carbon accumulation in Chinese croplands. *Proc. Natl. Acad. Sci. USA* **2018**, *115*, 4045–4050. [CrossRef] [PubMed]
24. Zhang, H.; Ouyang, Z.; Jiang, P.; Li, M.; Zhao, X. Spatial distribution patterns and influencing factors of soil carbon, phosphorus, and C:P ratio on farmlands in southeastern China. *Catena* **2022**, *216*, 106409. [CrossRef]
25. Li, T.X. *Report of China's National Dialogue on Food Security and Sustainable Development for the United Nations Food Systems Summit (Chapter 6)*; United Nations: New York, NY, USA, 2021; pp. 327–328.

26. Liu, F.; Wu, H.; Zhao, Y.; Li, D.; Yang, J.L.; Song, X.; Shi, Z.; Zhu, A.-X.; Zhang, G.L. Mapping high resolution National Soil Information Grids of China. *Sci. Bull.* **2022**, *67*, 328–340. [CrossRef]
27. Zhou, T.; Geng, Y.; Ji, C.; Xu, X.; Wang, H.; Pan, J.; Bumberger, J.; Haase, D.; Lausch, A. Prediction of soil organic carbon and the C: N ratio on a national scale using machine learning and satellite data: A comparison between Sentinel-2, Sentinel-3 and Landsat-8 images. *Sci. Total Environ.* **2021**, *755*, 142661. [CrossRef]
28. Zhou, T.; Geng, Y.; Chen, J.; Pan, J.; Haase, D.; Lausch, A. High-resolution digital mapping of soil organic carbon and soil total nitrogen using DEM derivatives, Sentinel-1 and Sentinel-2 data based on machine learning algorithms. *Sci. Total Environ.* **2020**, *729*, 138244. [CrossRef]
29. Shangguan, W.; Dai, Y.; Liu, B.; Ye, A.; Yuan, H. A soil particle-size distribution dataset for regional land and climate modelling in China. *Geoderma* **2012**, *171–172*, 85–91. [CrossRef]
30. Yan, F.; Shangguan, W.; Zhang, J.; Hu, B. Depth-to-bedrock map of China at a spatial resolution of 100 meters. *Sci. Data* **2020**, *7*, 2. [CrossRef] [PubMed]
31. Zhang, M.K. Soil clayization and argic horizon identification in mountain and hilly areas of southern China. *J. Agric.* **2021**, *11*, 53–57, (In Chinese with English abstract).
32. Xie, H.H.; Wu, Q.G.; Hu, J.Y.; Yu, L.F.; Bie, P.F.; Wang, H.; Deng, D.Z. Changes in soil physical and chemical properties during the process of alpine meadow degradation along the eastern Qinghai-Tibet Plateau. *Eurasian Soil Sci.* **2018**, *51*, 1440–1446. [CrossRef]
33. Halecki, W.; Kruk, E.; Ryczek, M. Loss of topsoil and soil erosion by water in agricultural areas: A multi-criteria approach for various land use scenarios in the Western Carpathians using a SWAT model. *Land Use Policy* **2018**, *73*, 363–372. [CrossRef]
34. FAO; IIASA; ISRIC; ISS-CAS; JRC. *Harmonized World Soil Database (Version 1.1)*; FAO: Rome, Italy; IIASA: Laxenburg, Austria, 2009.
35. Lan, J. *Comparison Characteristics of Weathering Degree, Clay Minerals and Iron Oxides of Carbonate Weathering Crusts at Different Altitude in West Yunnan-Guizhou Plateau*; Yunnan Normal University: Kunming, China, 2021; (In Chinese with English abstract).
36. Cai, Y.F. *Enrichment and Distribution of Pedogenic Iron Oxides and Its' Climatic and Tectonic Significance in Yunnan-Guizhou Plateau*; Southwest University: Chongqing, China, 2021; (In Chinese with English abstract).
37. Guo, S.; Cai, Y.; Ren, J.; Guan, Y.; Xin, D.; Long, X. Formation and migration of magnetic particles associated with iron oxide transformation at a hillslope scale. *Catena* **2021**, *197*, 104944. [CrossRef]
38. Zhang, F.R.; Huang, Q.; Zhang, D. The significance of clayey layer, Its criteria for series classification in the nouth china plain. *Chin. J. Soil Sci.* **2001**, *5*, 197–200, (In Chinese with English abstract).
39. Yi, W.; Wang, S.; Yang, S.; Zhao, H.; Jin, X.; Wang, G. Humus distribution and forms in the sediments from shallow lakes in the middle and lower reaches of the Yangtze River. *J. Lake Sci.* **2011**, *23*, 21–28.
40. Xiang, T.T. *Studying on the Process of Erosion-Deposition of Eastern Slope of Great Khingan and Its Indicative Significance*; Jilin University: Changchun, China, 2014; (In Chinese with English abstract).
41. Duan, J.L.; Zhang, G.; Ren, Y.Y.; Zhang, X.L.; Li, W.D. Study on Interactive Relationship between Spatial Distribution Pattern of Soil and Surface Water. *Soils* **2021**, *53*, 1072–1080, (In Chinese with English abstract).
42. Gavinelli, F.; Fusaro, S.; Ivan, D.; Ragusa, S.; Paoletti, M.G. Unpredicted ecological and ecosystem services of biodiversity. Spontaneous vegetation, hedgerows, and maple trees as useful landscape components to increase predatory mite population in agroecosystems. *Appl. Soil Ecol.* **2020**, *154*, 103584. [CrossRef]
43. Dong, Y.; Yang, J.-L.; Zhao, X.-R.; Yang, S.-H.; Mulder, J.; Dörsch, P.; Peng, X.-H.; Zhang, G.-L. Soil acidification and loss of base cations in a subtropical agricultural watershed. *Sci. Total Environ.* **2022**, *827*, 154338. [CrossRef]
44. Ng, E.L.; Lwanga, E.H.; Eldridge, S.M.; Johnston, P.; Hu, H.W.; Geissen, V.; Chen, D. An overview of microplastic and nanoplastic pollution in agroecosystems. *Sci. Total Environ.* **2018**, *627*, 1377–1388.
45. Hughes, P.; McBratney, A.B.; Huang, J.; Minasny, B.; Micheli, E.; Hempel, J. Comparisons between usda soil taxonomy and the australian soil classification system i: Data harmonization, calculation of taxonomic distance and inter-taxa variation. *Geoderma* **2017**, *307*, 198–209. [CrossRef]
46. Esfandiarpour-Borujeni, I.; Mosleh, Z.; Farpoor, M.H. Comparing the ability of soil taxonomy (2014) and wrb (2015) to distinguish lithologic discontinuity and an abrupt textural change in major soils of iran. *Catena* **2018**, *165*, 63–71. [CrossRef]
47. Weng, H.L.; Ci, E.; Lian, M.S.; Chen, L.; Hu, J. The origin of acidic purple soil in chongqing and its significance for soil genetic classification. *J. Southwest Univ.* **2019**, *41*, 32–39, (In Chinese with English abstract).